December 2008 *Volume 2 Issue (2-3)*

Trade Science Inc.

Nano Science and Nano Technology

An Indian Journal

Full Paper

NSNTAIJ, 2(2-3), 2008 [87-93]

Simulation and analysis of electrical conductance of carbon nanotubes

Neeraj Jain*, Harsh

Solid State Physics Laboratory, DRDO, Delhi, (INDIA)

E-mail : njainsspl@gmail.com

Received: 22nd September, 2008 ; Accepted: 27th September, 2008

ABSTRACT

Carbon nanotubes (CNTs) show great promise as a new class of electronic materials owing to a control on their electrical properties with chirality of the nanotube. On one hand, they can rival the best metal as an interconnect and on the other, a semiconducting nanotube can work as a channel in a nano field effect transistor. The energy band structure and density of states of single wall nanotubes (SWNTs) with different chiralities is reviewed here and then using a diameter dependent model, the electrical conductance of a SWNT, a multi wall nanotube (MWNT) and bundle of CNTs containing MWNTs is simulated and analyzed. It is found that conductance of a CNT depends largely on its geometry. An MWNT shows very high conductance which varies with average tube diameter, length and number of shells in the tube. Similarly, we can play with the conductance of a CNT bundle by varying its dimensions and density of nanotubes inside the bundle. This study would play an important role in understanding the working of various CNT based electronic devices.

1. INTRODUCTION

Carbon nanotubes (CNTs) were discovered in 1991 by Sumio Iijima[1] and since then they have turned into a hot area of research activity, fuelled by experimental breakthroughs that have led to realistic possibilities of using them in a host of commercial applications like field emission based flat panel displays, semiconducting devices, hydrogen storage and ultra-sensitive chemical and electromechanical sensors.

In microelectronics, the scaling of devices has led to the desire to use nanowires in terms of vias, interconnects, field effect transistors (FETs) and memory elements. Carbon nanotube having huge current-carrying capacity, high mechanical and thermal stability is identified as an ideal component to be used in two main areas of integrated circuits (1) as an interconnect between the transistors and (2) as the channel material in FETs[2-7]. Experiments and theories have revealed that the electrical properties of carbon nanotubes can match or even exceed that of the best metals and semiconductors known. To use CNTs in various electronic devices or applications, it is essential to understand their basic electrical properties. In this paper, we report the dependence of electrical conductance of CNTs on their geometry and analyse the conductance of SWNTs and MWNTs[8-10].

2. Structure of single wall carbon nano tubes

A single-wall carbon nanotube is a rolled-up seamless cylinder of graphene sheet made of benzene-type hexagonal carbon rings with diameter of the order of a nanometer. Multi wall nanotubes are rolled-up stack of graphene sheets in concentric cylinders. Thus, a SWNT consists of one shell whereas a MWCNT has multiple number of shells. Depending on the direction in which the graphene sheet is rolled up (chirality), CNT demonstrates either metallic or semi-conducting properties. Three types of nanotubes are possible, called armchair, zigzag and chiral nanotubes, depending on how the two-

Full Paper

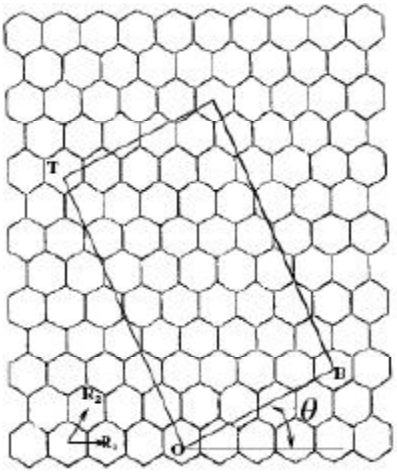

Figure 1 : Depiction of a graphite sheet for [3, 2] nanotube

dimensional graphene sheet is "rolled up".

As single-walled CNT can be constructed conceptually by rolling up a single sheet of graphite along one of its 2 D lattice vectors B = nR1 + mR2 to form a nanotube with diameter D = $a[3(n^2 + nm + m^2)]^{1/2}/\pi$ and chiral angle$\theta = \arctan(\sqrt{3}m/[2n + m])$[11,12] where a = 1.421 Å is the carbon-carbon-atom distance in a graphite sheet. It is convenient to specify CNT in terms of a pair of integers[n,m]. When m = 0, a type of CNT classified as zigzag tube is formed whose diameter D = $\sqrt{3}na/\pi$ and chiral angle $\theta = 0^o$ and an armchair tube with diameter D = $3na/\pi$ and chiral angle $\theta = 30^o$ is obtained by taking n = m. All other nanotubes, with chiral angles intermediate between 0° and 30° are chiral nanotubes.

An example of a chiral[2,3] nanotube is shown in figure 1. The vector T is the 1D translation vector ($T = t_1R_1 + t_2R_2$) of the nanotube along the axis. The unit cell marked as the rectangle involves $4(n^2 + nm + m^2)/d$ atoms with d the highest divisor of (2n+m, 2m+n)[11,12].

The remarkable property of SWNTs is that their electrical nature is determined by the values of n and m. They show metallic properties when n=m or n-m is multiple of 3 and semi-conducting behaviour when n-m is not a multiple of 3.

3. Energy dispersion diagrams and electronic density of states of SWNTs

In a nanotube, electrons in the circumferential direction are confined in the tube. So the circumferential component of the wave vector, which satisfies the periodic boundary condition, can only take the values fulfilling the condition $k.B_{ch} = 2\pi q$ where q is an integer. The allowed energy states of the tube are cuts of the graphene band structure. When these cuts pass through a Fermi point (K point of the first Brillouin zone), the tube is metallic. In cases where no cut passes through a K point, the tubes are semiconducting.

In the energy band diagrams, the N^{th} band in CNT is equivalent to its I^{st} band. So zone folding method is used to find the energy dispersion diagram of CNT from that of 2D graphene[11]. This gives the energy dispersion relation as

$$\mathbf{E_q(k) = E_g^{2D}[\,k\,(K_2/|K_2|) + q\,K_1]\ where}$$
$$\mathbf{q = 0,1,2\ldots.N\text{-}1\ and\ -\pi/T < k < \pi/T} \qquad \mathbf{(1)}$$

where $K_1 = (-t_2\,b_1 + t_1\,b_2)/N$ and $K_2 = (mb_1 - nb_2)/N$ are reciprocal lattice vectors of CNT and $b_1 = 2\pi\,i/3a + 2\pi\,j/v3a$ and $b_2 = 2\pi i/3a - 2\pi\,j/\sqrt{3}a$ are reciprocal lattice vectors for 2D graphene and E_g^{2D} is the energy dispersion relation of 2D graphite which (using tight binding calculation) is given by

$$\mathbf{E_g^{2D}(k_x,k_y) = \pm\gamma_0\,(1 + 4\cos(3k_xa/2)\cos(\sqrt{3}k_ya/2) + 4\cos^2(\sqrt{3}k_ya/2))^{1/2}} \qquad \mathbf{(2)}$$

where γ_0 is the nearest neighbor transfer integral (also called the hopping matrix element) and its value is found to lie between 2.5-3.2 eV.

The electronic density of states are obtained from the energy dispersion relation.

$$\mathbf{DOS(E) = 2/\pi\,\Sigma\int|\partial E_{CNT}/\partial k_t|^{-1}\,dE_{CNT}} \qquad \mathbf{(3)}$$

Case I

For armchair CNTs, m=n and k_x is in the circumferential direction. Applying the boundary condition $3nak_x = 2\,\pi\,q$, $|T| = v3\,a$ in eqn.(2), we get

$$\mathbf{E_q^{armchair}(k) = \pm\gamma_0\,(1 + 4\cos(\pi\,q/n)\cos(\sqrt{3}ka/2) + 4\cos^2(\sqrt{3}ka/2)^{1/2}}, \qquad \mathbf{(4)}$$

where q = 0,1, … n ; $-\pi/\sqrt{3}a < k < \pi/\sqrt{3}a$

There are n+1 dispersion relations for both conduction and valence bands. Out of these (n+1) relations two bands are nondegenerate and the rest n-1 are doubly degenerate. The lowest conduction band and the highest valence band are found to cross each other (figure 2a) at the fermi level. This signifies that all armchair tubes are metallic in nature. The DOS diagram (figure 2b) also shows the presence of states at the fermi energy.

Case II

For zigzag CNTs, m=0 and k_y is in the circumferential direction. So, after applying the boundary condi-

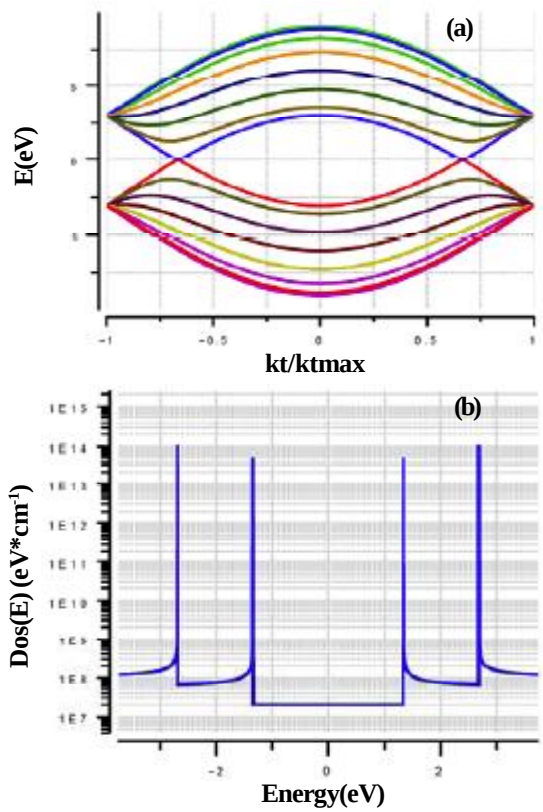

Figure 2: Energy band diagram and density of states for (7,7) CNT Metallic in nature

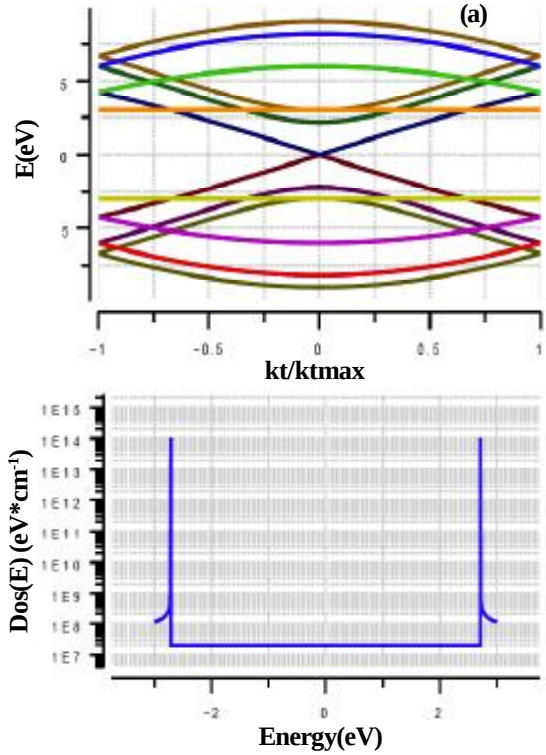

Figure 3 : Energy band diagram and density Of states for (6,0) CNT semi-metallic in nature

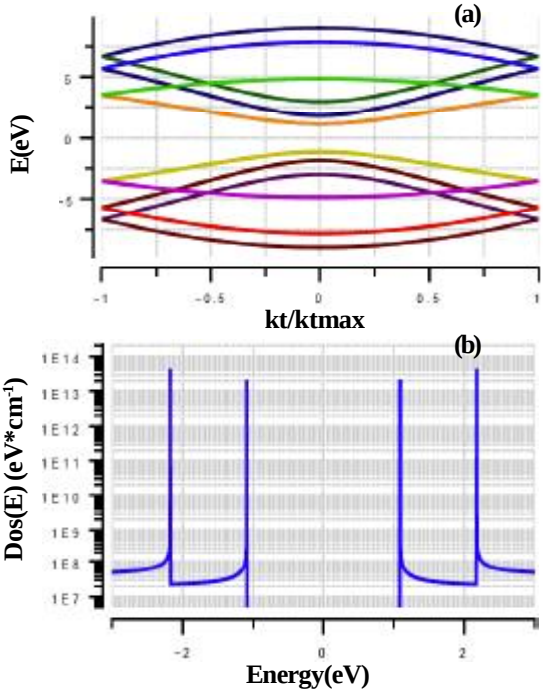

Figure 4: Energy band diagram and Density Of States for (5,0) CNT semiconducting in nature

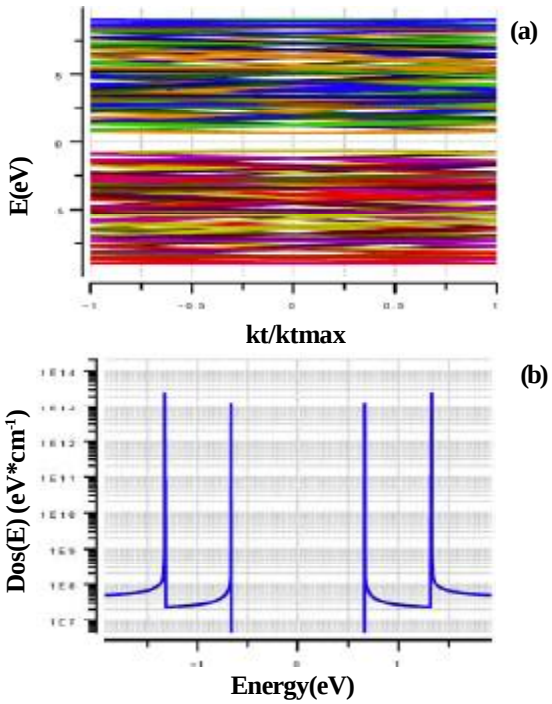

Figure 5 : Energy band diagram and Density Of States for (7,2) CNT semiconducting in nature

tion $\sqrt{3}nak_y = 2\pi q$, $|T| = 3a$ in eqn.(2), we get

$$E_q^{zigzag}(k) = \pm \gamma_0 (1 + 4\cos(\pi q/n)\cos(3ka/2) + 4\cos^2(\pi q/n)^{1/2} \quad (5)$$

where $q = 1, \ldots 2n$; $-\pi/3a < k < \pi/3a$

Full Paper

The band diagram shows that there is negligible gap between the lowest conduction band and highest valence band when n is a multiple of 3 (figure 3a) and definite no. of states are present at the fermi energy (figure 3b), in which case CNT is metallic or semimetallic in nature. There exists a gap when n is not a multiple of 3 and it behaves as a semiconductor (figure 4a).

Case III

In Chiral CNTs also, the band diagram shows a gap at the fermi level when n is not a multiple of 3 and a semiconducting behaviour is depicted (figure 5a) but in case, n is a multiple of 3 then CNT shows a metallic behaviour.

The density of states at Fermi level is zero for semiconducting CNTs whereas it has a definite value for metallic CNTs. The difference between the two peaks on both the sides of the fermi energy gives the value of the energy band gap for semiconducting CNTs which can be written as $E_g = 2a\,\gamma_0/d$ which shows that the energy band gap varies inversely with tube diameter (d).

4. Conductance of carbon nanotubes

Most existing studies have shown that individual SWNTs suffer from a high ballistic resistance of approximately 6.5kΩ though they have electron mean free paths of the order of a micron[13]. According to the recent findings, all shells in a MWNT can conduct if they are properly connected to the contact, leading to a very low overall resistance[14]. A 25 μm long MWNT with an outer diameter of 100nm is shown to have an overall resistance of 35Ω[15]. This is a significant improvement over the early experimental results of resistance values in KΩ/MΩ ranges where only one outer shell in a MWNT conducts[16]. Bundles of these CNTs in parallel can provide very high conductance[3-6].

CNT conductance model

The conductance of a carbon nanotube is obtained using the two-terminal Landauer-Buttiker formula. This formula states that, for a 1-D system with N channels in parallel, the conductance $G=(Ne^2/h)T$,

where T is the transmission coefficient for electrons through the sample[13]. Due to spin degeneracy and sublattice degeneracy of electrons in graphene, each nanotube has four conducting channels in parallel (N=4). Hence the conductance of a single ballistic SWNT assuming perfect contacts (T=1), is $4e^2/h = 155\mu S$, which yields a resistance of 6.45 KΩ[13]. This is the fundamental resistance associated with a SWNT that cannot be avoided[16,17]. This fundamental resistance is equally divided between the two contacts on either side of the nanotube.

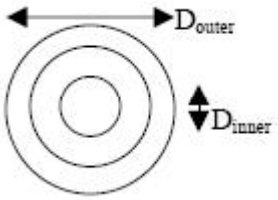

Figure 6 : Cross-section of MWNT

An earlier conductance model[18] expresses the conductance per channel as:

$$G=G_0/(1+l/\lambda) \quad (5)$$

where G_0 is quantum conductance, l is the length of CNTs and λ is the mean free path. This equation leads to different conductance values according to different l values (for $l<\lambda$) e.g. for $l = 0.5\lambda$, $G = 0.667G_0$ and $G = 0.556G_0$ for $l = 0\lambda$.

These values are inconsistent with the ballistic properties of CNTs. The ballistic conductance of the CNT should be a constant for any value of $l < \lambda$ [10-14]. Therefore, the model of[18] based on eqn. (5) was modified by Wei wang et al.[19] to provide an accurate conductance analysis of the nanotubes.

According to this model, the conductance of a MWNT or a SWNT is determined by two factors: the conducting channels per shell and the number of shells. A SWNT consists of 1 shell whereas in a MWCNT, the number of shells is diameter-dependent, i.e.

$$N_{shell} = 1+[(D_{outer} - D_{inner})/2\delta]$$

where δ=0.34nm is the Vander Waals distance, D_{outer} and D_{inner} are the maximum and minimum shell diameters respectively. Thus, the diameter of each shell is

$$d_i = D_{inner} + i\times 2\delta \text{ , where } i = 0, 1, \ldots, Nshell-1 \quad (7)$$

Assuming the metallic tube ratio is r, the approximate number of conducting channels per shell is :

$$N_{chan/shell} = (ad+b)r \quad ; d>6 \text{ nm}$$
$$= 2r \quad ; d<6 \text{ nm} \quad (8)$$

where $a = 0.1836\ nm^{-1}$ and b = 1.275[11]

Generally, we have r = 1/ 3 in MWNT or a bundle of CNTs[11], then

$$N_{chan/shell} = (ad+b)/3 \quad ; d>6 \text{ nm}$$
$$= 2/3 \quad ; d<6 \text{ nm}$$

One conducting channel of the CNT will provide either intrinsic conductance (Gi) or Ohmic conductance (Go) according to the tube length l. For low bias situation (V_b <≈0.1V), the diameter-dependent channel conductance for one shell is given by

$$G_{shell}(d_i,l) = G_i N_{chan/shell}; l <= \lambda$$
$$= G_o N_{chan/shell}; l > \lambda \quad (9)$$

where the mean free path $\lambda = v_F d/\alpha t$ is diameter-dependent[19], α is the total scattering rate, t is temperature and v_F is the Fermi velocity of graphene.

Ohmic conductance $Go = 2q^2 \lambda/h$ l is diameter dependent[6], and the channel intrinsic conductance is a constant[19], i.e., $G_i = 2q^2/h = 1/12.9k\ \Omega$ (where h is Planck's constant, q the charge of an electron and l the tube length). Here, we consider the perfect contact and neglect the contact resistance since recently developed fabrication techniques can provide contacts with very small resistance values[14].

Using eqn.(9), the conductance of a metallic SWNT ($N_{chan/shell} = 2$) for diameter d (0.4nm < d< 4nm[6]) and a length l, is

$$G_{shell}(d,l) = 2 G_i ; l <= \lambda$$
$$= 2 G_o ; l > \lambda$$

consistent with the analysis in[3-6].

The number of shells in an MWNT is determined by D_{outer} based on eqn. (6). Each shell has its own d_i, λ and $N_{chan/shell}$, which are derived from D_{outer}.

Hence, the total conductance is the summation of conductance of all these shells:

$$G_{MW}(D_{outer},l) = \sum_{N_{shell}} G_{shell}(d_i, l) = \sum_{D_{inner}}^{D_{outer}} G_{shell}(d_i, l) \quad (10)$$

We have considered the conductance at room temperature T = 300K in the tube direction and the impact of inter-shell interaction[19] is not included. It can be seen from eqn. (10) that when the outer diameter of a MWNT increases and the number of shells remains the same, the conductance will gradually increase. As the outer diameter reaches a certain value, the MWNT will have one more shell and its conductance will increase dramatically. In case of CNTs with length larger than λ, the conductance starts to decrease due to the effect of Ohmic resistance.

Based on the above conductance estimation of both MWNT and SWNT (a special case of MWNT), the total conductance inside a mixed CNT bundle is obtained as

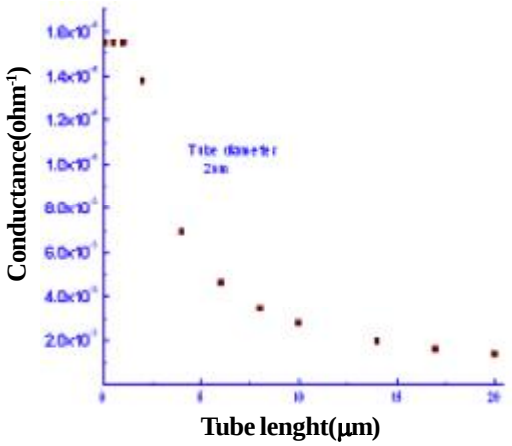

Figure 7 : Conductance v/s. Tube length (Metallic SWNT - diameter 2 nm)

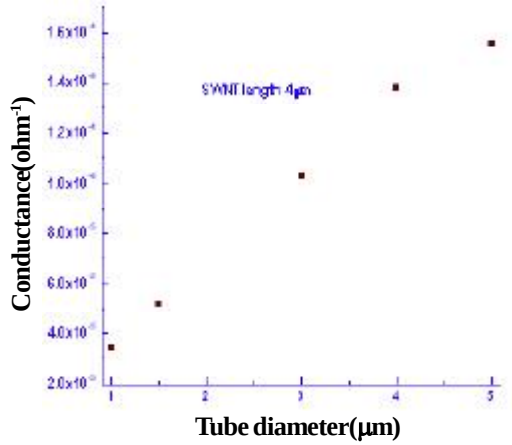

Figure 8 : Conductance v/s. Tube diameter (Metallic SWNT - length 4μm)

$$G_{bundle} = \int G_{MW}(D_{outer}, l)\, N(D_{outer})\, \partial D_{outer} \quad (11)$$

where $N(D_{outer})$ is the tube count and a normal (Gaussian) distribution with a mean diameter mD_{outer} and a standard deviation σ_{Douter}[14,15] is followed by the tubes in the bundle.

Assuming the total number of CNTs in the bundle as N_{bundle}, the tube count for a given D_{outer} is given by $N(D_{outer}) = N_{bundle}/\sqrt{(2\Pi)}\ \sigma_{Douter} * \exp(-1/2 *([D_{outer} - mD_{outer}]/\sigma_{Douter})^2)$ (12)

Based on eqn.(12), a distribution curve for the tube count is obtained. Using this distribution curve and the corresponding MWNT conductance curve, the total conductance of the mixed bundle is estimated using eqn.(12).

RESULTS AND DISCUSSION

The mean free path of electrons in a CNT is typically 1-2μm. For CNT lengths less than this, electron

Full Paper

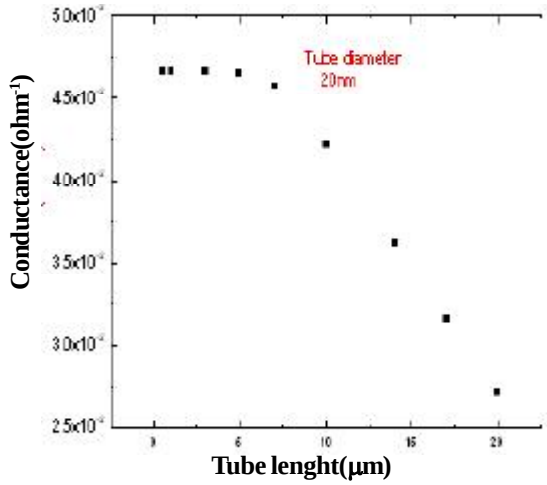

Figure 9 : Conductance v/s. Tube length (MWNT-diameter 20 nm)

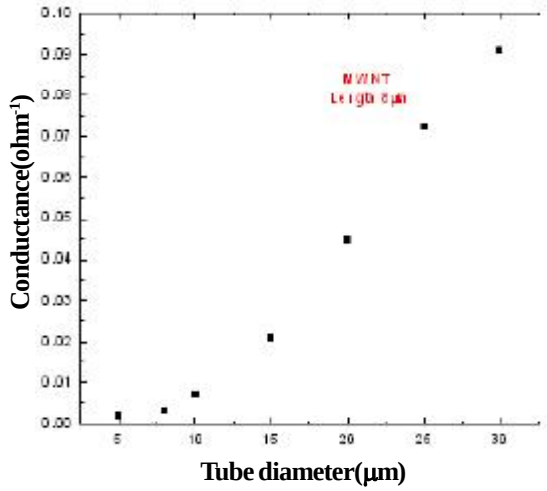

Figure 10 : Conductance v/s. Tube diameter (MWNT - length 8 μm)

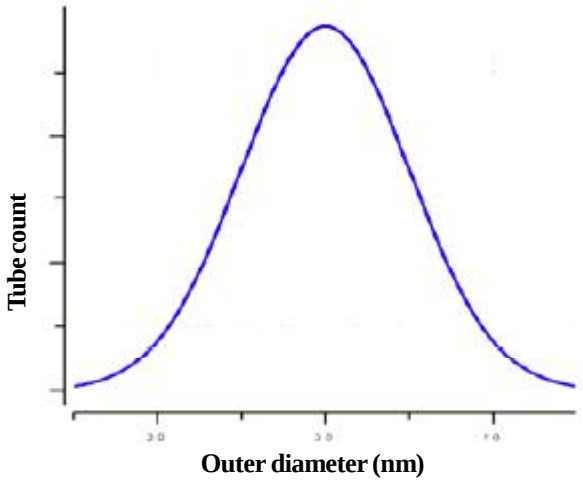

Figure 11 : Tube count v/s. Outer tube diameter

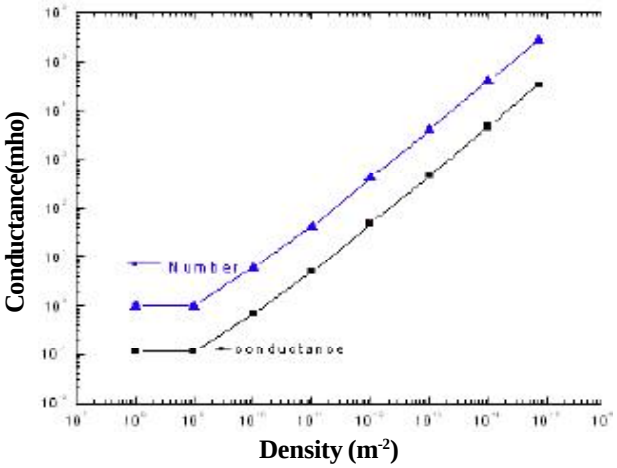

Figure 12 : Conductance v/s. Tube density

transport is essentially ballistic within the nanotube and the conductance is independent of length. However, for lengths greater than the mean free path, conductance decreases (resistance increases) with length of the CNT (figure 7). This has also been confirmed by experimental observations[16,20]. Figure 8 shows increase in conductance with diameter of SWNT.

Figure 9 shows variation in conductance of an MWNT with its length which follows the same pattern as SWNT. However, in case of MWNT, the mean free path is found to be more than that of SWNTs. Figure 10 shows variation in conductance with diameter of MWNT. We see that conductance increases with increase in tube diameter because a MWNT of bigger diameter has more number of shells and hence more number of conducting channels which give rise to the increased conductance.

To estimate the conductance of CNT bundles, we need to specify parameters like bundle width, height and length; average diameter of the CNTs, standard variation in the diameter and also D_{inner}/D_{outer} apart from density of CNTs in the bundle and their probability of being metallic (r).

The sample CNT bundle with cross section area: $1\mu m^2$; length: 8μm; density: $\sim 10^{14}$ tubes/m^2 and average tube diameter of 30μm, $D_{inner}/D_{outer} = 0.5$ and probability of 90% of the tubes to be metallic was considered for conductance calculation. Assuming the tube count distribution versus D_{outer}, a normal distribution (figure 11) with mean diameter $mD_{outer} = 30nm$ and standard deviation $\sigma_{Douter} = 5nm$, the conductance of each CNT inside the bundle varies according to its outer diameter. Using eqn. (11), the total conductance was obtained as $4.683849\Omega^{-1}$ for r = 0.9 which is equiva-

lent to a resistance of 0.2134996Ω.

Other bundles with same parameters but of length (<8um) also give the same conductance and resistance value showing that till 8μm this bundle shows the minimum resistance. For different bundles this length can be different, beyond which if we increase the length, the conductance decreases. If a bundle is taken with more cross section area, the number of tubes in the bundle increases giving rise to increase in conductance. Similarly, predictably increasing the tube density in the bundle will increase the total number of tubes and hence the conductance as shown in figure 12.

The D_{inner}/D_{outer} ratio impacts the bundle conductance through changing the number of shells of MWNTs. A smaller value leads to more shells and a higher conductance. It is seen that for short tube lengths ($l<\lambda$), the conductance increases dramatically when l increases. When $l>\lambda$, l has modest effect on conductance improvement because the CNTs show ohmic resistance for the length beyond several micrometers.

5. CONCLUSION

The above study provides an estimation of conductance for different geometries of both MWNT as well as SWNT. In practice, the observed d.c. resistance of a CNT (at low bias) may be much higher than the resistance derived due to the presence of imperfect metal-nanotube contacts which give rise to an additional contact resistance. The total resistance of a CNT is then expressed as the sum of resistances arising from three aspects : the fundamental CNT resistance, scattering resistance and the imperfect metal-nanotube contact resistance. The total resistance may become very high so as to mask the observation of intrinsic transport properties of a CNT. The observed resistance for CNTs has typically been in the range of 100 KΩ although the lowest observed resistance is of the order of 7 KΩ approaching the theoretical limit[14].

This study would aid in observation of the change in conductance of nanotubes under different atmospheric conditions and while using these nanotubes in practical electronic devices. For realizing an interconnect using CNTs, it would be a good idea to use MWNTs or a bundle of CNTs as the resistance associated with an isolated CNT is too high to work effectively as an interconnect.

REFERENCES

[1] S.Iijima; Nature, **354**, 56 **(1991)**.
[2] 'International Technology Roadmap for Semiconductors', http://public.itrs.net, **(2005)**.
[3] K.Banerjee, S.Lin, N.Srivastava; Proc.Conf.on Asia South Pacific design automation.Japan, **(2006)**.
[4] M.Nihei, M.Horibe, A.Kawabata, Y.Awano; Proc.of the IEEE Inter.Interconnect Tech.Conf., 251-253 **(2004)**.
[5] A.Naeemi, R.Sarvari, J.D.Meindl; IEEE Elec.Dev. Lett., **26**, 84-86 **(2005)**.
[6] A.Raychowdhury, K.Roy; IEEE Trans. On Computer-Aided Design of Integrated Circuits and Systems, **25(1)**, 58-65 **(2006)**.
[7] D.H.Robertson, P.W.Brenner, J.W.Mintmire; Phys.Rev.B, 4512592 **(1992)**.
[8] R.A.Jishi, J.Bargin, L.Lou; Phys.Rev.B, **59**, 9862 **(1999)**.
[9] R.A.Jishi et al.; J.Phys.Soc.Japan, **63**, 252 **(1994)**.
[10] C.T.White, D.H.Robertson, J.W.Mintmire; Phys. Rev.B, **47**, 5485 **(1993)**.
[11] R.Saito, M.Fujita, G.Dresselhaus, M.S.Dresselhaus; Appl.Phys.Lett., **60**, 2204 **(1992)**.
[12] J.W.Mintmire, B.I.Dunlap, C.T.White; Phys.Rev. Lett., **68**, 631 **(1992)**.
[13] J.Li, Q.Ye, A.Casssell, H.T.Ng, R.Stevens, J.Han, M.Meyyappan; Appl.Physc.Lett., **82(15)**, 2491-2493 **(2003)**.
[14] S.Sato et al; Inter.Interconnect Tech.Conf., 230-232 **(2006)**.
[15] H.J.Li, W.G.Lu, J.J.Li, X.D.Bai, C.Z.Gu; Phys.Rev. Lett., **95(8)**, 86601 **(2005)**.
[16] J.W.Mintmire, C.T.White; Phys.Rev.Lett., **81**, 2506 **(1998)**.
[17] J.X.Cao, X.H.Yan, J.W.Ding, D.L.Wang; J.Phys. Condens.Matter, **13**, L271-L275 **(2001)**.
[18] A.Naeemi, J.D.Meindl; IEEE Elec.Dev.Lett., **27(5)**, 338-340 **(2006)**.
[19] Sansiri Haruehanroengra, Wei Wang; Electron Device Letters, IEEE, **28(8)**, 756-759 **(2007)**.
[20] A.Nieuwoudt, Y.Massoud; IEEE Trans.on Electron Devices, **53(10)**, 2460-2466 **(2006)**.
[21] L.Zhu, J.Xu, Y.Xiu, Y.Dennis, W.Hess, C.P.Wong; Carbon, **44**, 253-258 **(2006)**.
[22] C.L.Cheung, A.Kurtz, H.Park, C.M.Lieber; J. Phys. Chem., 2429-2433 **(2002)**.
[23] P.L.McEuen, M.S.Fuhrer, H.Park; IEEE Trans. Nano., **1(1)**, 78-85 **(2002)**.
[24] E.Brown, L.Hao, J.C.Gallop, J.C.Macfarlane; Appl. Physc.Lett., **87**, 023107 **(2005)**.